Regenerative Therapy 27 (2024) 290–300

Contents lists available at ScienceDirect

Regenerative Therapy

journal homepage: http://www.elsevier.com/locate/reth

Original Article

# Systemic investigation of di-isobutyl phthalate (DIBP) exposure in the risk of cardiovascular via influencing the gut microbiota arachidonic acid metabolism in obese mice model

Min Liu, Xifeng Du, Huifang Chen, Chenkai Bai, Lizhen Lan*

*Department of General Practice, First Hospital of Shanxi Medical University, No.85, Jiefang South Road, Taiyuan, Shanxi, 030001, China*

ARTICLE INFO

*Article history:*
Received 2 February 2024
Received in revised form
17 March 2024
Accepted 24 March 2024

*Keywords:*
Phthalate esters
DIBP
Metagenomics
Arachidonic acid
Cardiovascular diseases

ABSTRACT

Phthalate esters (PE), a significant class of organic compounds used in industry, can contaminate humans and animals by entering water and food chains. Recent studies demonstrate the influence of PE on the development and progression of heart diseases, particularly in obese people. Di-isobutyl phthalate (DIBP) was administered orally to normal and diet-induced obese mice in this research to assess cardiovascular risk. The modifications in the microbial composition and metabolites were examined using RNA sequencing and mass spectrometry analysis. Based on the findings, lean group rodents were less susceptible to DIBP exposure than fat mice because of their cardiovascular systems. Histopathology examinations of mice fed a high-fat diet revealed lesions and plagues that suggested a cardiovascular risk. In the chronic DIBP microbial remodeling metagenomics *Faecalibaculum rodentium* was the predominant genera in obese mice. According to metabolomics data, arachidonic acid (AA) metabolism changes caused by DIBP were linked to unfavorable cardiovascular events. Our research offers new understandings of the cardiovascular damage caused by DIBP exposure in obese people and raises the possibility that arachidonic acid metabolism could be used as a regulator of the gut microbiota to avert related diseases.



## 1. Introduction

Phthalate esters (PE) are used in a wide variety of industrial applications. PE was used in a wide variety of sectors depending on their density. Due to their great tensile strength, high density PE is used to make water pipelines, detergent bottles, garbage cans, and milk bottles. Toys, adhesives, plastic bottles, containers, tubes, and bulletproof materials are all made with ultra-high-density PE. They are also employed for prosthetic joints and implants in hip and knee surgery due to their strong chemical resistance. Grocery bags, cables, wrapping paper, saran wrap, home goods, and squeeze bottles are all made of low-density PE. DIBP is a crucial PE component found in products including nail polish, lubricants, beauty products, paints, inks, and lacquers. They are added as softeners to provide flexibility [1]. Because the phthalate esters are not covalently attached to the products they are used in, they can leach into the environment. Di-isobutyl phthalate (DIBP) is a chemical that belongs to the phthalate ester class and is generally not toxic, but high exposure levels can have dangerous health effects. DBP (Dibutyl phthalate) and DIBP both have detrimental effects on the developing male genital system [2]. DIBP is ubiquitous in a number of environmental matrices, including sediment, water, and air. It is known that some aquatic species bioaccumulate DIBP. But the likely effects of DIBP on obese people need to be further understood.

According to studies on mammals, PE can cause a variety of fertility issues in males, including abnormalities in reproductive development, steroid hormone imbalances, developmental toxicity, systemic inflammation, testicular lesions, and infertility

*Abbreviations:* PE, Phthalate esters; DIBP, Di-isobutyl phthalate; AA, Arachidonic acid; DBP, Dibutyl phthalate; ND, Normal diet; HFD, High-fat diet; CMC-Na, Sodium carboxymethylcellulose; TC, Total cholesterol; TG, Triglycerides; LDL-C, Low-density lipoprotein cholesterol; HDL-C, High-density lipoprotein cholesterol; FFA, Free fatty acids; IL-6, Interleukin (IL)-1β; TNF, Tumor necrosis factor; ROS, Reactive oxygen species; TMAO, Trimethylamine N-oxide.

* Corresponding author.
*E-mail address:* lanlizhen@sydyy.com (L. Lan).

Peer review under responsibility of the Japanese Society for Regenerative Medicine.

https://doi.org/10.1016/j.reth.2024.03.024

[3,4]. In *Caenorhabditis elegans*, phthalate esters are known to have neurotoxic effects [5]. Phthalate esters reduce heart rate in goldfish.

DBP and DIBP exposure in zebrafish disrupts spermatogenesis and causes toxic effects on male reproduction [6]. Free radicals, malondialdehyde, and 8-hydroxydeoxyguanosine were all increased in *Eisenia fetida* after subjection to DIBP. Additionally, it activated glutathione S-transferase activity and inhibited superoxide dismutase, catalase, and peroxidase [7]. Phthalates are primarily to blame for testicular dysfunction, ovarian toxicity, and a decrease in steroidogenesis in both humans and animals [8]. At the molecular level, there have been reports of potential reproductive toxicity [9]. In F1 larvae, disruption of molecular functions included binding of unfolded proteins, binding of E-boxes, and photoreceptor activity [10]. Comparison of the *in vitro* cytotoxicity of dibutyl phthalate and diisobutyl phthalate were done on skin and lung origin cells [11,12,28–30]. PE induces an increase in WBC count in the blood. PE raises weight and lowers zinc levels in the liver. PE, also known as endocrine disruptors, results in human spermatogenesis suppression and raised testosterone levels. Human colorectal cancer Caco-2 and HT-29 cell *in vitro* studies of PE revealed enhanced ROS generation in mitochondria through the destruction of DNA. In streptozotocin induced diabetic rats a sesquiterpene trilactone compound called bilobalide lowers blood glucose and increases the retina thickness by decreasing the oxidative stress [13]. Higher levels of pro-inflammatory secretions by PE raise the risk of cancer. PE exacerbated genomic instability in human peripheral blood cells even at low concentrations. Additionally, there was more evidence of increased micronucleation in the PE treated cells. PE slows down the growth process in endothelial progenitor cells and bone marrow. Furthermore, PE alters immune function and causes autoimmune diseases. PE poisoning is most frequently accompanied by IBS, or inflammatory bowel syndrome. Neurotransmitters in the brain are harmed by PE, which also raises the possibility of neoplasia. The gut microbiota improves the immunity of the host and gut dysbiosis leads to various ageing and longevity related problems [14]. Last but not least, prolonged exposure to PE results in organ malfunction and inflammation [15–17].

Epidemiological and experimental data on DIBP's effects on cardiovascular health are lacking, but given its rising environmental concentration and clear toxicity, it is urgent to learn more about the toxin's effects and how it contributes to cardiovascular diseases, particularly in vulnerable populations.

Gut remodeling is one of the powerful techniques to analyze the changes in the intestinal flora according to the toxin exposure. The entire bacterial flora changes indicate the exact changes and pathways involved in the exposure of the toxin. Small molecules known as metabolites are created throughout the metabolic process. Metabolites can be either the final or intermediate molecule in a process. These tiny compounds make it possible to analyze metabolomics with high throughput. In order to diagnose biomarkers, it is helpful to understand the molecular mechanisms underlying the process through the identification and changes in the metabolites. The research aids in identifying the ideal therapeutic target for any diseases or toxicities. Environmental toxicants have been the subject of numerous metabolomics research. Using the metabolomics investigation, the impacts of environmental toxicants were examined on a number of model species [18,19]. In this work, gut microbiota modeling caused by DIBP toxicity and associated metabolites were investigated. Using a mice model, the alterations in the arachidonic acid system were examined, along with their relationship to cardiovascular disorders. Arachidonic acid (AA) pathway lipid metabolism and immunity were linked to various cardiovascular diseases. It also shows link with obesity and fatty liver diseases. The majority of body cells' cell membranes contain arachidonic acid, a polyunsaturated fatty acid that is covalently bonded in an esterified state. After an injury or irritation, arachidonic acid is liberated and oxygenated by enzyme systems, which results in the production of eicosanoids, a significant class of inflammatory mediators. The work's potential applications include figuring out how organ damage and metabolites relate to biomarkers.

In order to study the cardiotoxicity of DIBP on obese and normal individuals, an experimental mice model was developed. Then, 16S rRNA gene sequencing and untargeted metabolomics analysis were used to investigate the gut microflora profile and metabolic homeostasis. Metagenomics and metabolomics analysis were performed to screen potential bacteria and metabolic pathways. The results were then *in vitro* validated. Here in this study the toxicity of DIBP related to cardiovascular diseases are studied in mice along with its gut modelling and metabolomics.

## 2. Materials and methods

### 2.1. Chemicals

DIBP (CAS#84-69-5) (Sigma-Merck), DL-4-chlorophenyl alanine (CAS#7424-00-2) (Sigma–Aldrich), 1-[bis(dimethylamino)methylene]- 1H-1,2,3-triazolo [4,5-b] pyridinium 3-oxide hexafluorophosphate (HATU) (CAS#148893-10-1) (Sigma–Aldrich), Triethylamine (TEA, HPLC Grade) (CAS#121-44-8) (Sigma–Aldrich), 1-hydroxy benzotriazole hydrate (HOBt) (CAS#123333-53-9) (Sigma–Aldrich) and Cholamine chloride hydrochloride (CAS#3399-67-5) (Sigma–Aldrich). Polyunsaturated fatty acids (PUFAs) mixed standards were purchased from Universal Biologicals (Cambridge, UK).

### 2.2. Animals and DIBP exposure

Eighty male C57BL/6 mice were purchased from the Experimental Animal Center of Guangzhou University of Chinese Medicine. Eight to ten weeks old mice were taken for the study. All mice after acclimatization were split into different groups of 30 mice each. High-fat diet (HFD) was given to create obese model to weigh more than the normal ones and normal diet (ND) was given to others [20] (Table 1). DIBP was dissolved in sodium carboxymethylcellulose (CMC-Na) (0.3%) (CAS#9004-32-4) (Sigma–Aldrich, St. Louis, MO, USA) at a concentration of 300 mg per kg (low), 500 mg per kg (medium), and 1000 mg per kg (high). The normal and obese groups were further divided into four sub-groups. One sub-group was control (0.3% CMC-Na) (oral gavage) (ND-C/HFD-C group), and the remaining groups were low (ND-L/HFD-L), medium (ND-M/HFD-M) and high (ND-H/HFD-H) DIBP concentrations for 10 weeks as mentioned earlier. Mice were euthanized by isoflurane and the Institutional Animal Care and Use Committee (IACUC) protocols were followed for the animals.

**Table 1**
Composition of Normal (ND) and High-fat diet (HFD) of mice.

| Nutrients | %/100g | Nutrients | %/100g |
|---|---|---|---|
| Carbohydrate | 43 | Carbohydrate | 48.8 |
| Protein | 17 | Protein | 21 |
| Fat | 40 | Fat | 3 |
| Ingredients | g/100g | Calcium | 0.8 |
| Powdered rat feed | 68 | Phosphorous | 0.4 |
| Maize oil | 6 | Fibre | 5 |
| Ghee | 6 | Moisture | 13 |
| Milk powder | 20 | Ash | 8 |
| Total energy (kcal/100g) | 414 | Total energy (kcal/100g) | 306.2 |

### 2.3. Assessment of heart rate, glucose, lipids, and cytokine levels

Blood was drawn from the mice after a 14-hour fast, and fasting blood glucose levels were assessed using a blood glucose meter (ACCU-CHEK Performa, Roche, Switzerland). The mice's heart rates were continuously recorded using a MiniTR (Nanjing, China) monitor. Weekly urine and stool samples were taken, along with measurements of body weight. Following ten weeks of treatment, all mice were killed, and blood and tissue samples were taken. To obtain the supernatants for biochemical analysis, mice blood samples were centrifuged at 3500 rpm for 15 min at 4 °C. Using Total cholesterol (TC), triglycerides (TG), low-density lipoprotein cholesterol (LDL-C), high-density lipoprotein cholesterol (HDL-C), and free fatty acids (FFA) kits (Rongsheng Biological Co., Ltd., China) the serum lipids level were determined.

The murine ventricular function was using a Vevo 3100 ultra high-resolution ultrasound imaging (Fujifilm Limited, Toronto, Canada). The extent of murine heart injury was assessed using the doppler images. IL-1β, 6, and TNF-α levels were assessed using ELISA kits (Wuhan Huamei Biotechnology) under the manufacturer's recommendations. Reactive oxygen species (ROS) were measured using a ROS assay kit from the Beyotime Institute of Biotechnology in China. Following the method from Chen K et al. [21], plasma TMAO levels Cui A [22] were examined using liquid chromatography coupled with triple-quadrupole mass spectrometry.

### 2.4. Heart tissue hematoxylin and eosin and masson staining

The heart was excised into segments that were 5 μm long and fixed in paraffin after being fixed in the Bouin solution (4% paraformaldehyde) (Sigma-Merck). After that, the cells were stained following industry protocol using hematoxylin and eosin (SBT10001; Sunteambio Biotechnology, Shanghai, China) and a masson dye solution set (Servicebio).

### 2.5. Profiling of gut microbiota

Using a ZR fecal DNA kit (D6010; Zymo Research Corp., Orange, CA), fecal DNA was extracted from about 50 mg of feces using mechanical lysis of the cells and silica column purification. To remove humic acids and polyphenols a double step of pre-washing and washes was performed. DNA concentration was determined using QuantiFluor's dsDNA System (Promega, Madison, WI) and 1 μg of DNA was taken for microbial profiling. Using degenerate primers 338F (5′-ACTCCTACGGGAGGCAGCAG-3′) and 806R (5′-GGACTACHVGGGTWTCTAAT-3′) and a PCR thermocycler 9700(ABI, CA, USA), amplicons of the 16S rRNA V3–V4 region were produced. The paired-end sequencing was done using the Illumina platform NexSeq 550 series (Illumina, USA). In a metagenomic sequencing analysis, DNA fragments with an average size of 400 bp were obtained using the Covaris M220 (Gene Company Limited, China), and a paired-end library was then constructed using NEXTflexTM Rapid DNA-Seq (Bioo Scientific, Austin, TX, USA). The constructed 16S metagenomic libraries were purified using AxyPrep Mag PCR Clean-up kit. Using a Bioanalyzer 2100 usi DNA 7500 chips (Agilent Technologies, USA), library quality control was done. USEARCH was utilized to quality filter the raw sequences and UPARSE was utilized to cluster the unique sequences (OTU) at 97% similarity. RDP Classifier (version 2.2) was used to compare the taxonomy of each OTU representative sequence to the 16S rRNA database using a confidence threshold of 0.7.

### 2.6. Untargeted metabolite profiling

Fecal samples were weighted and combined with an extraction solvent (acetone: ethanol: water = 2:2:1) after being freeze-dried. As the internal standard, 4-chlorophenyl alanine was utilized. After homogenizing the samples, they were submerged three times in ice and centrifuged. The centrifuged liquid was dried in a nitrogen dryer and again redissolved in ethanol–water (1:1). Using methanol and dichloromethane (3:1), the precipitate was extracted. Equal volumes of all collected supernatants were made as quality control (QC) samples.

The extracts were separated on an XB-C18 column (Phenomenex Kenetix 2.6 μm, Torrance, CA, USA), and the untargeted metabolomics were performed using ultra-high performance liquid chromatography with quadrupole time-of-flight mass spectrometry (UPLC-Q-TOF-MS)equipped with a shimadzu-30A LC system (Shimadzu, Kyoto, Japan) Triple TOF™5600$^{+}$ mass spectrometry equipped with electro spray ionization (ESI) (AB Sciex, USA). In contrast to mobile phase B, which was acetonitrile, mobile phase A for chromatography is composed of 0.1% formic acid in water for positive mode and 5 mM ammonium acetate in water for negative mode. The gradient began at 1% B and in 25 min rose to 100% B.

The drying gas and sheath gas temperatures were set at 300 °C and 375 °C, respectively. The voltage of the fragmentor was set at 150 V, and the nebulizer pressure was set at 35 psig. The column's temperature was maintained at 45 °C. The injection volume was 10 μL, and the flow rate was 0.3 mL/min. High-purity nitrogen was used at constant flow rates of 8 L/min and 12 L/min, respectively, as a drying gas and sheath gas.

### 2.7. Targeted analysis of arachidonic acid metabolism

The derivatization method was utilized to analyze the targeted metabolomics of arachidonic acid metabolism. A 1.5 mL tube was filled with the internal standard solution containing prostaglandin D2-d4 and dried under N2. The frozen ethanol/water (4:1) mixture was added along with the fecal sample, and the mixture was then homogenized for 2 min. The supernatant was obtained following a 5-min incubation period on ice and a 5-min centrifugation at 13,500 rpm. The precipitate was removed in the similar manner. Both the supernatants were dried in a nitrogen dryer and taken for derivatization.

### 2.8. Arachidonic acid degradation by Faecalibaculum rodentium

*F. rodentium* anaerobic bacteria were acquired from the RIKEN BioResource Research Center (Tsukuba, Ibaraki, Japan) and inoculated in modified PYG mediumat 120 rpm for 1–2 days at 37 °C. The PYG medium was spun at 1500 g for 10 min, they were washed in 0.9% NaCl. Using an AnaeroPack (ThermoScientific, Massachusetts, USA), the reaction blend (0.1 M phosphate buffer (pH 7.2) and 0.2/0.4/1 mg/mL arachidonic acid) was thoroughly mixed with the obtained species in an anaerobic system. 50 μL of the centrifuged sample was mixed with equal proportion of cold ethyl acetate and isopropanol, then centrifuged once more for 5 min at 13,000 rpm. Targeted metabolomics-like derivatization techniques were employed for analysis.

### 2.9. Statistical evaluation

Unpaired t-test was employed to find the statistical difference. Results were interpreted as 95% confidence mean intervals.

Standard deviation (SD) was used for *in vitro* experiments, non-targeted metabolomics, and arachidonic acid metabolism. NDA (Normal Discriminant Analysis) was employed to differentiate groups. By using Spearman's correlation tests, correlation analyses were evaluated.

## 3. Results

### 3.1. Assessment of heart rate, glucose, lipids, and pro-inflammatory cytokines

After the DIBP exposure period, the heart rates were lower in the HFD-H group (Fig. 1A). In ND rodents, there were no discernible variations between the control and treated groups. As explained by the temporal analysis (Fig. 1B), the heart rate increased in the initial four weeks, and decreased from the fifth week(0.95-fold, $p < 0.05$) to tenth week(0.92-fold, $p < 0.001$). The blood sugar levels of the DIBP treatment groups were higher (Fig. 1C). Consequently, it raises the chance of developing prediabetes. As seen in Fig. 1D, the HFD-H group had significantly lower levels of high-density lipoprotein cholesterol (HDL-C) (2.395 ± 0.395 mM, $p < 0.01$) and elevated TC and TG are 1.465 ± 0.405 mM, $p < 0.05$ and 5.355 ± 0.705 mM, $p < 0.001$ respectively. Obese mice individuals had elevated inflammatory factors (IL-1β, IL-6, and TNF-α) levels than the ND group, and it appeared that DIBP had an impact on these levels (Fig. 1F). Mice fed DIBP for 10 weeks showed noticeably higher plasma TMAO levels than control mice fed DIBP-free food (Fig. 1G).

Heart oxidative stress was looked at consecutively to further investigate the negative effects of DIBP. The DCF fluorescence assay was utilized to gauge the cardiac ROS level by DIBP in mice. The result shows a definite rise in ROS levels in rodents fed DIBP, while control rodents not given DIBP showed no appreciable differences.

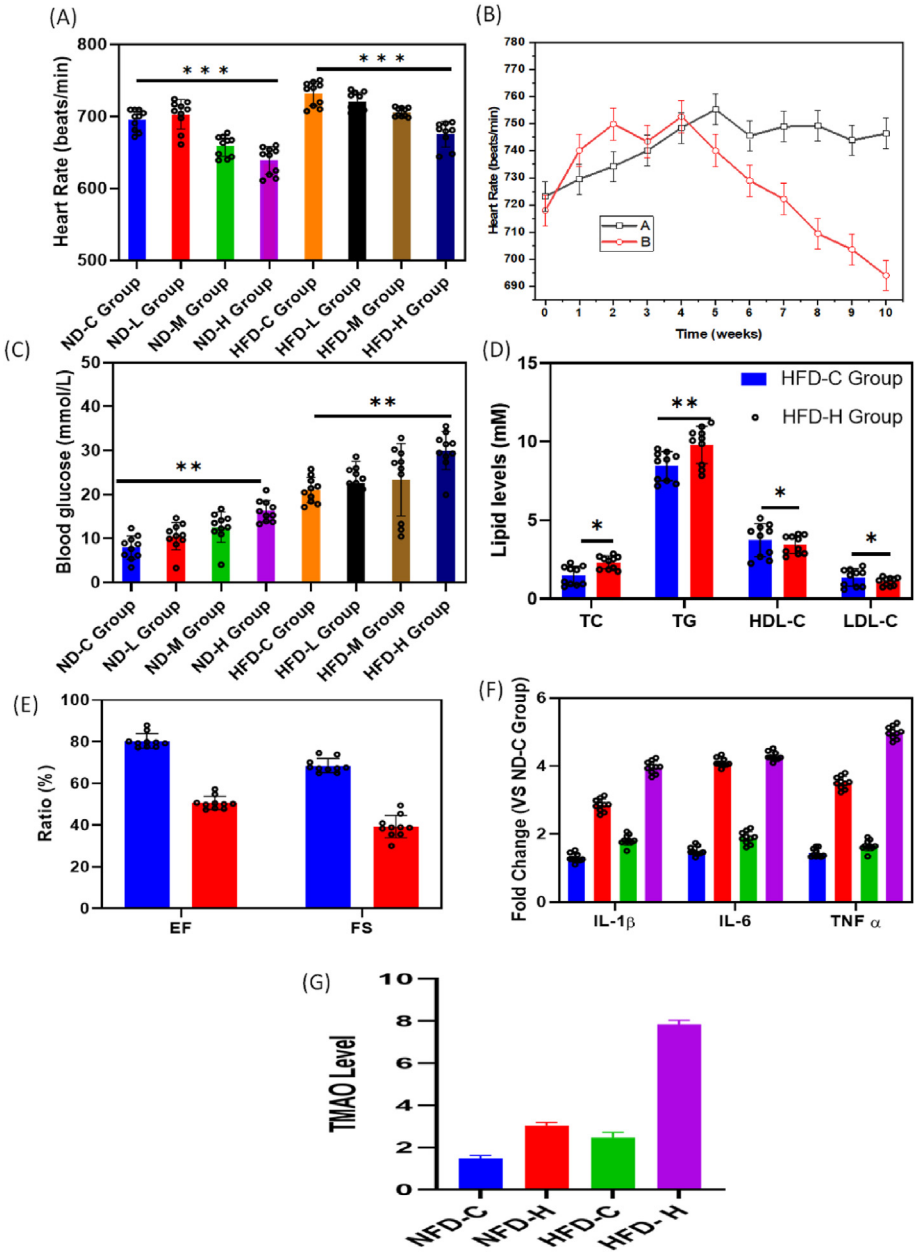


**Fig. 1.** Effects of DIBP exposure on cardiovascular health (A) Heart rate (B) Heart rate from 0 to 10 weeks (C) Blood glucose level (D) TC, TG, HDL-C and LDL-C levels (E) Ultrasound indicators (F) Inflammation factors (G) TMAO level. Values are mean with a 95 % confidence interval of ten mice.

The mice's heart was examined using ultrasound technology, and the HFD-H group had lower ejection fraction (EF) and fractional shortening (FS) values than the HFD-C group (Fig. 1E).

It was evident that the high level of DIBP caused an influx of inflammatory cells, which further supported the induction of inflammation and severe fibrosis in obese mice. DIBP also induced coronary heart disease (CHD) in treated mice and sudden death. The inflammation, fibrosis and coronary heart disease were demonstrated by H&E and Masson staining (Fig. 2A and B).

### 3.2. Profiling of gut microflora

The fecal pellets from 10-week DIBP exposed mice were analyzed by 16s rRNA sequencing for gut microbial remodeling. The Venn diagram in Fig. 3A showed 83% OTU overlap between the control and treated groups, and there were 38 and 29 endemic species respectively. The interpretation of principal component analysis (PCA) separated the control and treated obese groups with reference to their gut microbial signatures. When compared to the control group, DIBP increased the ratio of *Helicobacter*, Lachnospiraceae, and *Dubosiella* while significantly reducing the ratio of Coriobacteriaceae and *Mucispirillum*(Fig. 3B).

The top genera according to the results of the NDA was the genus *Faecalibaculum* (Erysipelotrichaceae). By demonstrating a rise in lipid levels, an increase in inflammatory markers, a drop-in heart rate *Faecalibaculum* has been found to have the strongest association with an increased risk of cardiovascular disease among gut bacteria. The abundance of *F. rodentium* in the HFD mice was a strong indicator of DIBP-induced gut microbial remodeling (Fig. 3C).

The phylum *Firmicutes* (*Faecalibaculum*, *Lactobacillus*, and *Romboutsia*) became more abundant in DIBP exposure. In our study, it was discovered that *Faecalibaculum* elevates the lipids level and inflammatory factors and suppresses the heart rate of the obese mice. The aforementioned data represents that regardless of the

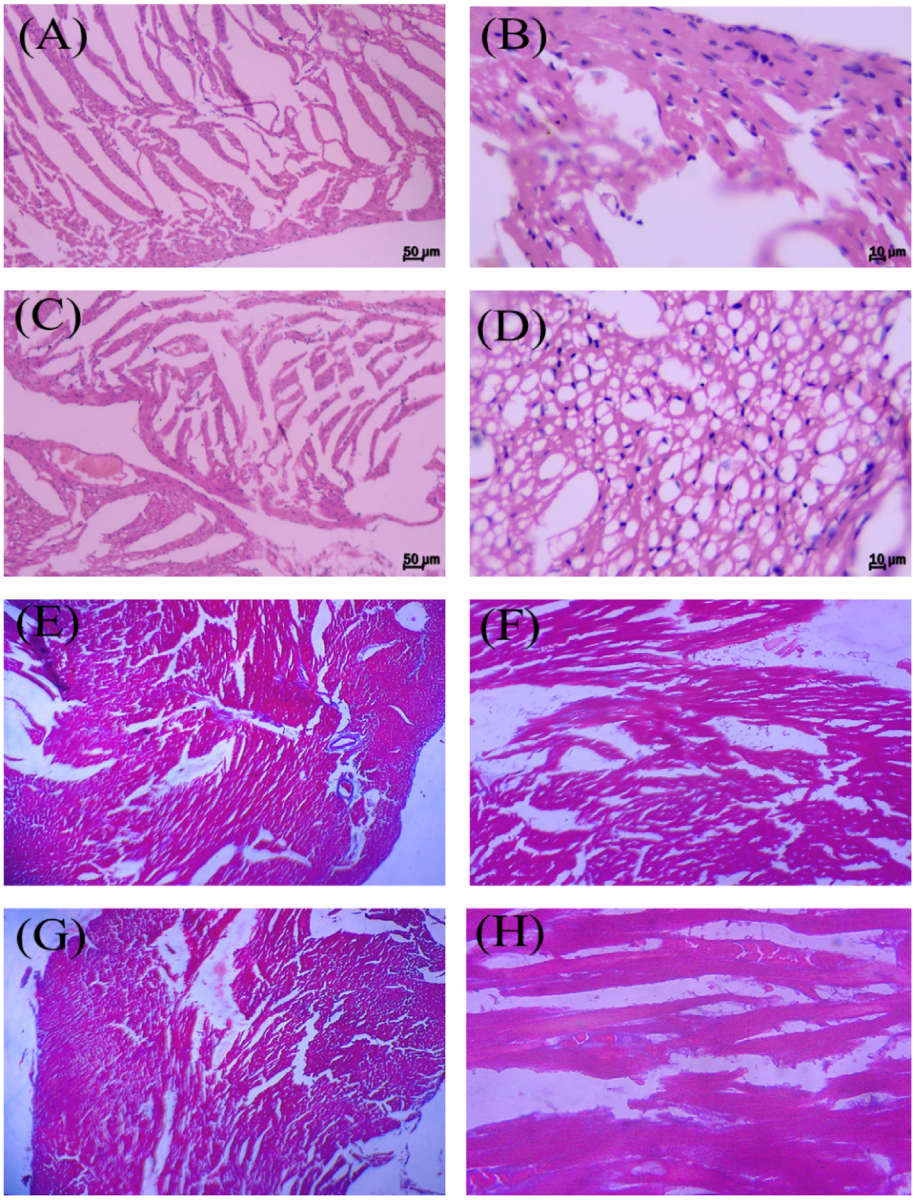


**Fig. 2.** a. H&E and Masson-stained heart sections (A&E) ND-C, (B&F) ND-H, (C&G) HFD-C, (D&H) HFD-H. b. Microscopic changes in coronary atherosclerosis. A1-control, B1- CHD (coronary heart disease) group, C1 & C2 – Intraplague bleeding, rupture and death group (HE staining, scale bar = 1 mm).

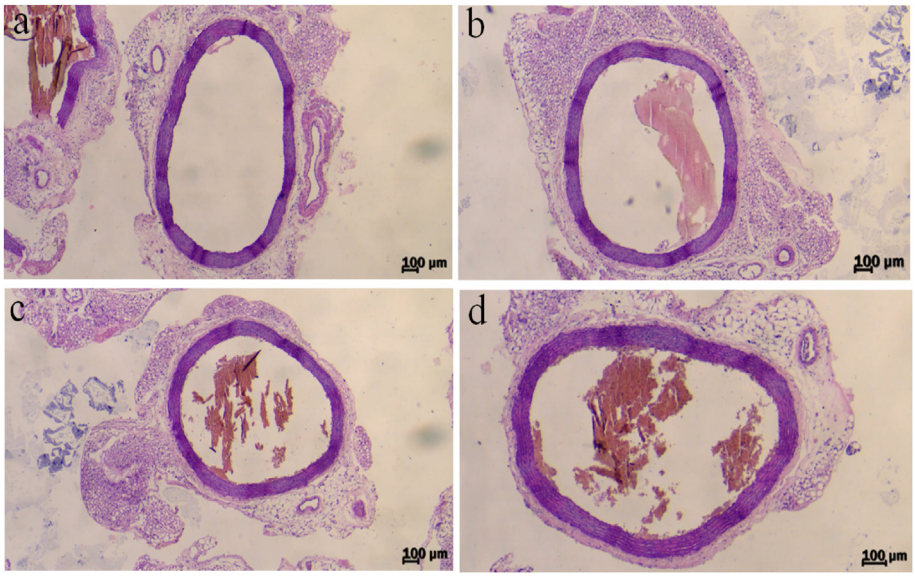


**Fig. 2.** (*continued*).

exact process is still unknown, we hypothesize that prolonged DIBP exposure and *F. rodentium* abundance due to gut remodeling will definitely increase the risk of heart related disorders in obese mice.

### 3.3. Untargeted metabolomics

UPLC-Q-TOF-MS was utilized to analyze the feces of the DIBP and non-DIBP groups. The feces samples showed 60 (55 up-regulated and 5 down-regulated) metabolites and 100 (62 up-regulated and 38 down-regulated) lipids. Additionally, we used partial least squares discrimination analysis (PLS-DA) to confirm that DIBP exposure changed the metabolites of the gut microbiota. Both the HFD-H and HFD-C groups displayed a unique metabolites and lipids patterns, as shown in Fig. 4. To avoid model overfitting in the various modes, the PLS-DA model's predictive abilities were assessed using a permutation test and seven-fold cross-validation. The determined metabolites revealed a connection with 26 pathways using the KEGG database. DIBP significantly impacted few pathways, including arachidonic acid, purine, butanoate, unsaturated fatty acid biosynthesis, arginine biosynthesis and linoleic acid. Arachidonic acid remained top among all the pathways. The overall metabolome of feces changes due to DIBP exposure showed that the arachidonic acid metabolism disruption results in those changes.

### 3.4. Targeted analysis of arachidonic acid metabolism

Cyclooxygenase (COX) (Prostaglandin G/H Synthase (PGHS)) enzyme converts arachidonic acid into prostaglandin H2 and prostaglandin G2 which serve as substrates for numerous downstream enzymes to produce prostaglandins (prostaglandin F2, prostaglandin E2, Prostaglandin I2, and thromboxane. These downstream metabolites were elevated in the prior untargeted study. But the leukotriene B4 was increased in the HFD-H group. Moreover, it was discovered that the availability of 5- lipoxygenase enzyme products had increased in the cytochrome P450 (CYP) pathway and the epoxyeicosatrienoic acids (5, 6- epoxyeicosatrienoic acids, 14, 15- epoxyeicosatrienoic acids) were down-regulated (Fig. 5). According to the correlation analysis leukotriene B4, 5-hydroxyeicosatetraenoic acids (5- hydroxyeicosatetraenoic acids), 11- hydroxyeicosatetraenoic acids, and 12- hydroxyeicosatetraenoic acids metabolites of lipoxygenase were positively correlated with *Faecalibaculum*, whereas epoxyeicosatrienoic acids (5, 6- epoxyeicosatrienoic acids, 14, and 15- epoxyeicosatrienoic acids) were negatively associated with *Faecalibaculum*. Prostaglandin I2 and Thromboxane A2 are primary prostanoids and functional cyclooxygenase pathway antagonists. The higher amounts of DIBP-induced leukotriene B4 and 5-hydroxyeicosatetraenoic acids showed a negative influence on cardiac function. Importantly, the metabolomics analysis revealed an

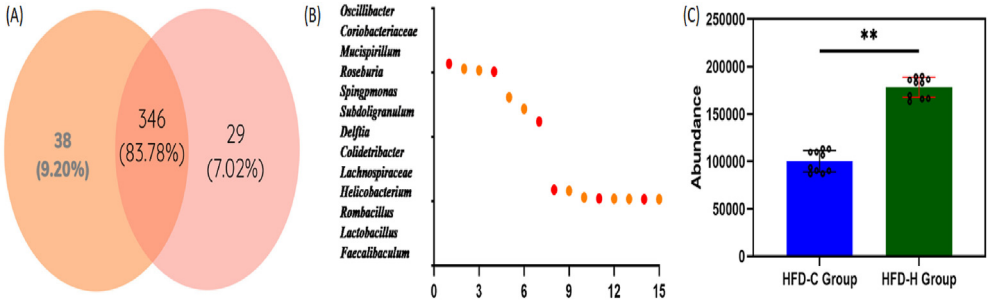


**Fig. 3.** Relative abundance and composition of gut bacteria in DIBP exposed obese mice (A) Venn diagram (B) Top 13 distinct bacterial genera identified by LEfSe analysis of their linear discriminative analysis (LDA) score (C) Abundance of *F. rodentium*. Data are presented as mean with a 95 % confidence interval for n = 10.

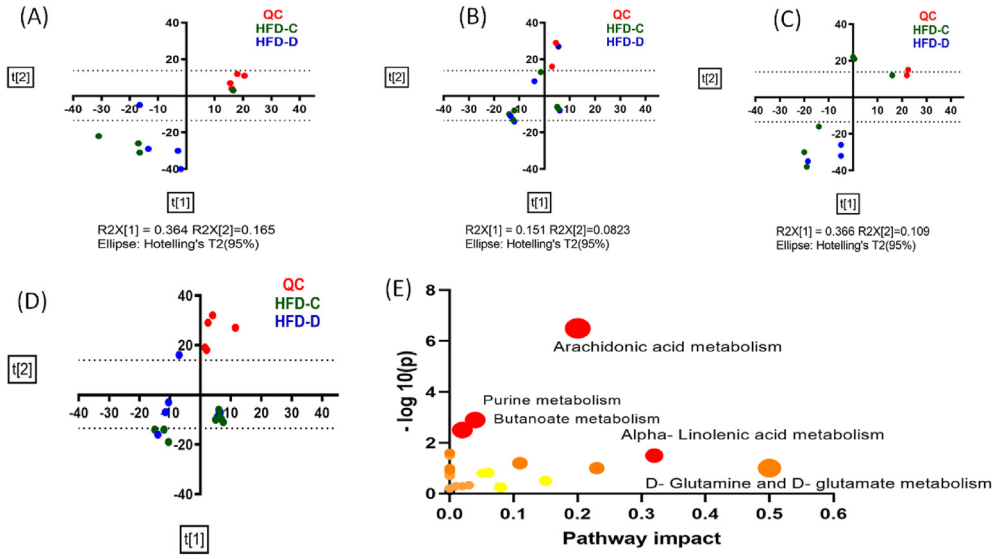


**Fig. 4.** Untargeted metabolomics profile of gut microbiota (A–D) PLS-DA score plots of fecal sample extracts: metabolomics analysis (A) positive ionization mode and (B) negative ionization mode; lipidomics analysis (C) positive ionization mode and (D) negative ionization mode (E) Pathway analysis of the significantly changed metabolites in the fecal sample metabolome and lipidome conducted using MetaboAnalyst.

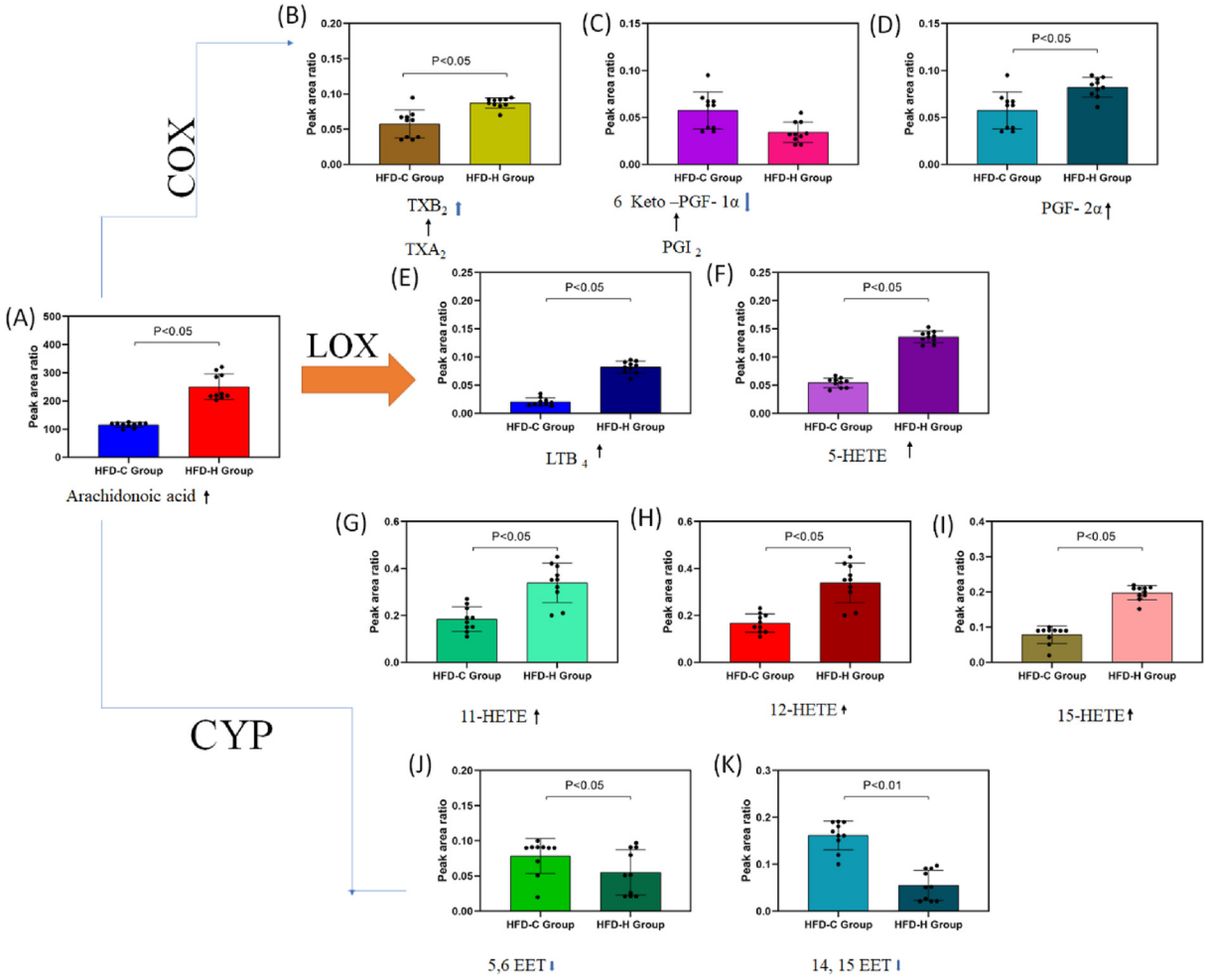


**Fig. 5.** Comparison of the concentrations of arachidonic acid and metabolites after DIBP exposure (A) arachidonic acid (B–D) COX pathway (E–I) LOX pathway and (J–K) CYP pathway. Data are presented as mean ± SD for n = 6.

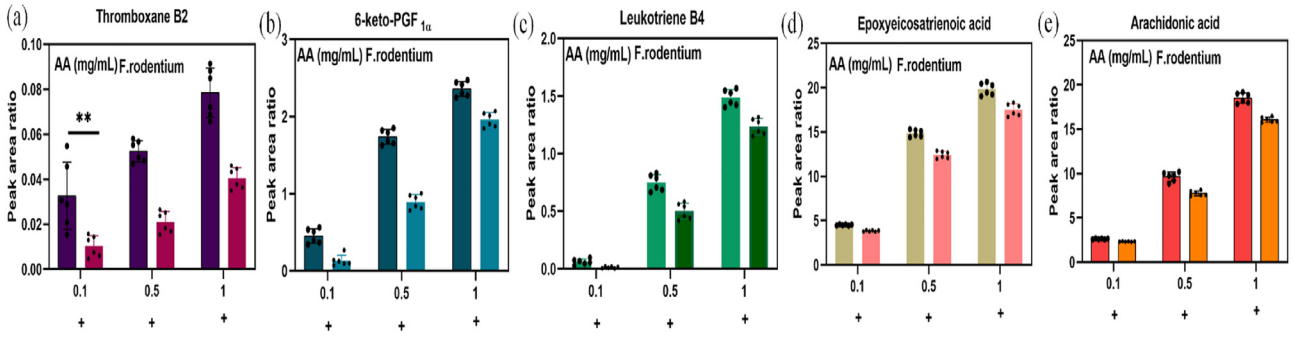


**Fig. 6.** *F. rodentium* modulated arachidonic acid metabolite levels (A&B) COX pathway (C) LOX pathway (D–E) CYP pathway. Blue columns, control groups (AA); Red columns, *F. rodentium* groups with AA. Data are presented as mean ± SD for n = 6.

increased detection of epoxyeicosatrienoic acids metabolites dihydroxyeicosatetraenoic acids.

### 3.5. *In vitroF. rodentium arachidonic acid degradation*

A different concentration of arachidonic acid (0.1, 0.5, or 1.0 mg/mL) substrate was included in *F. Rodentium* growth medium and maintained in an anaerobic environment. The proportion of thromboxane B2 and 6-keto-prostaglandin $F_{1\alpha}$, which are derivatives of Prostaglandin I2, were observed to be lower in the 0.1 or 0.5 mg/mL arachidonic acid groups compared to the control groups, but the thromboxane B2 decreased with increasing arachidonic acid dose. The only metabolite in the lipoxygenase pathway that was impacted by *F. rodentium* was leukotriene B4, and its abundance trend matched that of thromboxane B2. By including 1 mg/mL arachidonic acid the availability of 5, 6- epoxyeicosatrienoic acids, and 14, 15- epoxyeicosatrienoic acids in the CYP pathway was significantly reduced ($p < 0.05$ and $p < 0.01$) (Fig. 6). Arachidonic acid was dissolved in either potassium phosphate buffer or ultrapure water to check for spontaneous degradation since the mentioned metabolites were also in the untreated samples. Although arachidonic acid spontaneously degrades itself the visible differences in the metabolites suggests the relationship between *F. rodentium* and arachidonic acid. The change in the metabolic process and variations in the reaction environment prevents the identification of *F. rodentium* mechanism in the *in vitro* experiment.

## 4. Discussion

PE exposure has the probability to cause or worsen cardiovascular disease, being a health concern. By analyzing heart rate, heart tissue staining, blood glucose, plasma TMAO, and lipid profile in this study, we proved the DIBP impact on the obese mice heart tissues.

Phthalate esters (PEs), an organic pollutant, are frequently added in the manufacturing of plastics used to package food, cosmetics, and building materials [23]. PEs has non-covalent bonding and physicochemical characteristics and they can slowly exude from products and enter the environment [24]. The two most common PEs DBP and DIBP are ubiquitous in our environment like water and soil [25]. According to Kismali G [26], Tseng IL [5], and Sree CG [8], phthalates cause cancer, obesity, endocrine disorders, neuro cytotoxicity, and heart diseases.

The cytotoxic effects of phthalate metabolites on the lungs, kidneys, liver, and skin are also correlated to heart problems, coronary plagues, and hypertension [27,31]. Raised amounts of hs-CRP, fibrinogen, and D-dimer among individuals with congenital heart disease showed an atherothrombotic vulnerability correlated with exposure to bis (2-ethylhexyl) phthalate (DEHP) [32]. Heart rate is an alarming sign of total heart disease concern. The heart rate of HFD-H mice was lower than the HFD-C group, but no difference was seen in ND groups. Phthalate esters are thought to lower the cardiac rate in goldfish and cyprinodont fish, according to Pfuderer P [33,34]. Phthalates alter the heart rate via raising the blood pressure [35]. During the first four weeks of HFD-H DIBP treatment group, the pulse rate increased; however, in the fifth, eighth, and tenth weeks, it decreased. Similar studies have demonstrated that phthalate exposure increases the threat of cardiovascular related ailments by initially raising heart rate and subsequently lowering it [36]. Even though, obesity raises the pulse rate it got lowered in HFD group than the ND group [37]. Lipidomics study shows the DIBP influence on inflammatory processes and the function of leukocytes, and other immune cells including vascular and cardiac cells, and their effects on heart and its function.

Both DIBP exposure groups had higher blood glucose levels than the control groups. DEHP metabolites have been connected to glycemia, insulin resistance symptoms, and beta-cell health. Our findings give idea that exposure to phthalates may potentially affect blood glucose equilibrium and raise the chance of developing pre-diabetes [38]. Diethyl phthalate and dibutyl phthalate metabolites have been connected to high pregnancy glucose and pregnancy-related glucose intolerance [39]. According to Castro-Correia C (2018) and Elizabeth G. Radke [40,41], the possibility of developing metabolic syndrome like diabetes during pregnancy was highest for those who had exposure to DEHP, DBP, and DIBP [42,43]. While total cholesterol (TC) and triglyceride (TG) levels were significantly higher in the HFD-H DIBP treated group compared to the control group, high-density lipoprotein cholesterol (HDL-C) levels were significantly lower. A lower level of HDL-C was linked to phthalate [44]. The tests for inflammation and fibrosis, revealed that DIBP at higher levels caused a clear influx of inflammatory cells and severe fibrotic scarring in both obese and non-obese DIBP treated mice.

Intriguingly, DIBP exposure appeared to affect IL-1 β and TNF-α levels in obese people by increasing the levels. Phthalates are obviously known to increase inflammatory factors in older women. Monophthalates promote IL-6 and 8 synthesis in the *in vitro* human A549 epithelial cell line [45]. It was recently found that the exposure to phthalates at particular concentrations causes a diversity of cells, including macrophages and monocytes to secrete inflammation factors [46]. Ultrasound images showed lower heart automaticity in HFD-H groups. The results are consistent with those of earlier research in which the use of DEHP was found to impair cardiac automaticity [47,48]. In Comparison to control rodent given DIBP-free food, mice fed DIBP for 10 weeks displayed noticeably higher plasma TMAO levels. Cardiovascular and autoimmune diseases are directly correlated with elevated TMAO levels [49]. While the control mice showed no changes, the mice with DIBP had

elevated ROS levels. In Kunming mice, butyl phthalate induced ROS that damages the kidneys and liver and in earthworms ROS damages DNA [50]. By raising ROS, dibutyl phthalate also promotes mitophagy [51].

Gut microbiota is estimated as a vital indicator of external pollutants. The OTU overlap is nearly 83%.The intestinal bacteria differed between the treated and control groups, as resolved by principal component analysis (PCA). The highest score in the HFD-H group, as stipulated in the interpretation of the NDA comes under the genus *Faecalibaculum*(Erysipelotrichaceae). A heatmap association between *Faecalibaculum* and pathological factors demonstrates that the gut microbe is connected to high chance of heart disease. This heatmap showed an increase in lipid metabolism factors and inflammation factors and a decrease in heart rate. Similar work by Jonsson AL [52] also showed reduction in the butyrate producing intestinal flora in atherosclerosis. Together, the 16S rRNA-based sequencing and relationship interpretation disclosed the *Faecalibaculum* participation in the DIBP-induced gut remodeling. Deep metagenomic sequencing of fecal specimen revealed that *F. rodentium* predominated in the HFD-H samples. There are various fecal microbial forms in control and DIBP exposure groups. In a separate study, DEHP exposure increased Firmicutes while reducing Bacteroidetes (gram-negative anaerobes) [53]. Obesity in mammals has been connected directly to heart health by Firmicutes/Bacteroidetes [54]. We also noticed that phylum *Firmicutes* members were more prevalent after DIBP treatment. *F. rodentium* alters short-chain fatty acids profiles and causes free radical damage and inflammation. According to Brawner KM [55], *F. rodentium* lowers *Salmonella typhimurium* infection protection proteins while raising blood levels of IL-6. The findings imply that DIBP exposure increases the population of *F. rodentium* in HFD, which raises the cardiovascular risk.

By using UPLC-Q-TOF-MS, the metabolites of the gut microbiota were assessed for cardiovascular risks brought on by DIBP. The control and DIBP groups' feces samples contained 60 and 100 metabolites and lipids, respectively (data not shown). The gut microbiota metabolites that were altered by DIBP were examined using partial least squares discrimination analysis (PLS-DA), and were categorized based on their p-value, VIP, and fold change. The HFD-H and the HFD-C groups both displayed distinctive metabolite and lipid profiles on the PLS-DA score plots. 26 pathways were influenced in DIBP gut remodeling according to KEGG. Few pathways were indulged in DIBP gut remodeling, including arachidonic acid, purine, butanoate, α -linolenic acid, unsaturated fatty acid anabolism etc … Arachidonic acid remains the top among them. The untargeted metabolites study found eight metabolites were involved in the arachidonic acid process (data not shown). According to Higgins AJ [56], the arachidonic acid degradation was connected to inflammation, and Wang B [57] found that its metabolites were connected to cardiovascular diseases. It was previously understood that phthalate esters react with the enzymes cyclooxygenase, lipoxygenase and monooxygenase.

The quantity of arachidonic acid in targeted metabolomics was different in both control and treated. After DIBP exposure in the HFD mice, thromboxane B2 seemed to be overexpressed while 6-keto-prostagandin F1α (a derivative of (Prostaglandin I2 and Thromboxane A2) was downregulated. Similarly, prostaglandin F2α was significantly elevated following DIBP exposure. In the untargeted metabolomics investigation of the HFD-H group in comparison to the HFD-C group, it was also discovered that leukotriene B4lipoxygenase metabolite was increased [58]. Additionally, the 5- lipoxygenase enzyme seems to be increased. Epoxyeicosatrienoic acids also showed downregulation in the CYP pathway. According to correlation analysis, epoxyeicosatrienoic acids (5, 6- epoxyeicosatrienoic acids, 14, and 15- epoxyeicosatrienoic acids) were non-beneficially correlated with *Faecalibaculum* while leukotriene B4, 5-hydroxyeicosatetraenoic acids (5- hydroxyeicosatetraenoic acids), 11- hydroxyeicosatetraenoic acids, and 12- hydroxyeicosatetraenoic acids) of lipoxygenase were beneficially related with the bacterium. According to Weiss HJ [59], Prostaglandin I2 and Thromboxane A2 are vasoactive lipid messengers in the cyclooxygenase pathway, and they represent the danger of heart issues. Prostaglandin I2 to Thromboxane A2 conversion causes thrombotic diseases in heart attacks [60]. Therefore, the increased ratio of thromboxane B2/6-keto-prostaglandin F1α plays a part in heart related ailments caused by DIBP in HFD mice. Increased prostaglandin F2 levels raise heart rate and arterial blood pressure through cyclooxygenase enzymes or carbonyl reductase1 [61,62]. Increased levels of *leukotriene B4* and 5- hydroxyeicosatetraenoic acids, (neutrophil chemoattractants) by DIBP were reported in heart related diseases [63]. According to Huang CC [64,65], 5- hydroxyeicosatetraenoic acids increases the inflammation factors having cardioprotective properties like 11, 12, and 15- hydroxyeicosatetraenoic acids and epoxyeicosatrienoic acids levels (5, 6- epoxyeicosatrienoic acids, and 14, 15- epoxyeicosatrienoic acids) [66]. The intestinal bacterial remodeling by DIBP activates the enzyme soluble epoxide hydrolase for converting epoxyeicosatrienoic acids to dihydroxyeicosatetraenoic acids, a pro-inflammatory metabolite of epoxyeicosatrienoic acids.

Thromboxane B2 concentrations decreased whereas 6-keto-prostaglandin F1α concentrations increased by increasing arachidonic acid dose. *Leukotriene*B4 was the sole metabolite in the lipoxygenase pathway affected by *F. rodentium* and its abundance trend was same as thromboxane B2. The 1.0 mg/mL substrate inhibited the CYP pathways 5, 6, and 14- epoxyeicosatrienoic acids in the *F. rodentium* groups. Arachidonic acid undergoes non-enzymatic reactions when it interacts with reactive nitrogen species and molecular oxygen [67]. The cytochrome-encoding genes in the *F. rodentium* genome indicate the CYP function in the organism [68]. Furthermore, *F. rodentium* modifies IgA levels, which helps in the conversion of epoxyeicosatrienoic acids to dihydroxyeicosatetraenoic acids by elevating soluble epoxide hydrolase [69]. Autooxidation pathway might be the possible *in vitro* process. Furthermore, animal studies research can only reveal to a certain extent but the exact *in vivo* human body reaction to pollutants is to be considered.

Numerous tiny molecules, amino acids, lipids, carbohydrates, and other substances have been studied using metabolomics. The differences in metabolites enable researchers to learn more about the effects of a certain substance, toxins, or disease within a person. The understanding of metabolism-related ailments and diseases is made possible by the analysis of metabolites. The potential for studying and classifying a large number of metabolites explains the scope of metabolomics. Finding therapeutic targets for DIBP toxicity and the associated cardiovascular diseases will be the future focus of this study. The partial or peak overlaps of the metabolites, which require determining the coupling constants, are one of the study's limitations in the area of metabolomics. However, *in vivo* animal research clearly demonstrates that DIBP can cause problems with the cardiovascular system.

## 5. Conclusion

Overall,a drop-in heart rate, glycemia, elevated lipid levels and TMAO, inflammation, hepatocyte lipid accumulation, fibrosis, and plaque formation revealed the cardiovascular damage of prolonged DIBP exposed animals in this research. Obese individuals were more vulnerable to DIBP than normal mice regarding cardiovascular systems. Additionally, the multi-omics approach revealed that the altered metabolic equilibrium and gut microflora profile both significantly give rise to increased cardiovascular risk brought on by DIBP. *In vitro* culture studies were done to detect the *F. rodentium*

role on arachidonic acid process. These findings have important ramifications for our comprehension of how DIBP exposure led to cardiovascular harm in obese people and raise the possibility that the gut microflora arachidonic acid pathway is pivotal to DIBP-induced cardiovascular damage. Additional research is required to better understand the part of *F. rodentium* in gut remodeling and possible *in vivo* mechanisms.

## Data availability

The data used to support the findings of this study are available from the corresponding author upon request.

## Funding information

a. Shanxi Provincial Department of Science and Technology, Free Exploration Category, Project ID: 202203021211019.

b. Shanxi Provincial Study Abroad Office, Provincial Funding Program for Returned Overseas Scholars, Project ID: 2021-162.

c. Shanxi Medical University, 2022 Shanxi Province Higher Education Teaching Reform and Innovation Project (J20220324, General Project).

d. First Hospital of Shanxi Medical University, Youth Fund - 19.

e. Shanxi Provincial Department of Science and Technology, Natural Science Foundation, 2010011052-2.

f. First Hospital of Shanxi Medical University, Doctoral Research Fund-18.

## Declaration of competing interest

The authors compete no conflict of interest.

## References

[1] Yost EE, Euling SY, Weaver JA, Beverly BEJ, Keshava N, Mudipalli A, et al. Hazards of diisobutyl phthalate (DIBP) exposure: a systematic review of animal toxicology studies. Environ Int 2019;125:579–94. https://doi.org/10.1016/j.envint.2018.09.038.

[2] Borch J, Axelstad M, Vinggaard AM, Dalgaard M. Diisobutyl phthalate has comparable anti-androgenic effects to di-n-butyl phthalate in fetal rat testis. Toxicol Lett 2006;163(3):183–90. https://doi.org/10.1016/j.toxlet.2005.10.020.

[3] Corton JC, Lapinskas PJ. Peroxisome proliferator-activated receptors: mediators of phthalate ester-induced effects in the male reproductive tract? Toxicol Sci 2005;83(1):4–17. https://doi.org/10.1093/toxsci/kfi011.

[4] Howdeshell KL, Wilson VS, Furr J, Lambright CR, Rider CV, Blystone CR, et al. A mixture of five phthalate esters inhibits fetal testicular testosterone production in the sprague-dawley rat in a cumulative, dose-additive manner. Toxicol Sci 2008;105(1):153–65. https://doi.org/10.1093/toxsci/kfn077.

[5] Tseng IL, Yang YF, Yu CW, Li WH, Liao VHC. Phthalates induce neurotoxicity affecting locomotor and thermotactic behaviors and AFD neurons through oxidative stress in Caenorhabditis elegans. PLoS One 2013;9(6):e99945. https://doi.org/10.1371/journal.pone.0099945.

[6] Chen H, Chen K, Qiu X, Xu H, Mao G, Zhao T, et al. The reproductive toxicity and potential mechanisms of combined exposure to dibutyl phthalate and diisobutyl phthalate in male zebrafish (Danio rerio). Chemosphere 2020;258:127238. https://doi.org/10.1016/j.chemosphere.2020.127238.

[7] Yao X, Wang C, Li M, Jiao Y, Wang Q, Li X, et al. Extreme environmental doses of diisobutyl phthalate exposure induce oxidative stress and DNA damage in earthworms (Eisenia fetida): evidence at the biochemical and molecular levels. J Environ Manag 2023;331:117321. https://doi.org/10.1016/j.jenvman.2023.117321.

[8] Sree CG, Buddolla V, Lakshmi BA, Kim YJ. Phthalate toxicity mechanisms: an update. Comparative biochemistry and physiology. Toxicol Pharmacol: CB (Curr Biol) 2023;263:109498. https://doi.org/10.1016/j.cbpc.2022.109498.

[9] Chen H, Feng W, Chen K, Qiu X, Xu H, Mao G, et al. Transcriptomic analysis reveals potential mechanisms of toxicity in a combined exposure to dibutyl phthalate and diisobutyl phthalate in zebrafish (Danio rerio) ovary. Aquatic Toxicol (Amsterdam, Netherlands) 2019;216:105290. https://doi.org/10.1016/j.aquatox.2019.105290.

[10] Chang WH, Herianto S, Lee CC, Hung H, Chen HL. The effects of phthalate ester exposure on human health: a review. Sci Total Environ 2021;786:147371. https://doi.org/10.1016/j.scitotenv.2021.147371.

[11] Miranowicz-Dzierżawska K. Comparison of binary mixtures of dibutyl phthalate and diisobutyl phthalate cytotoxicity towards skin and lung origin cells in vitro. Toxicology 2023;486:153433. https://doi.org/10.1016/j.tox.2023.153433.

[12] Miranowicz-Dzierżawska K, Zapór L, Skowroń J, Chojnacka-Puchta L, Sawicka D. The effects of co-exposure to methyl paraben and dibutyl phthalate on cell line derived from human skin. Toxicol Res 2022;39(1):71–89. https://doi.org/10.1007/s43188-022-00151-3. PMID: 36721678.

[13] Su Q, Dong J, Zhang D, Yang L, Roy R. Protective effects of the bilobalide on retinal oxidative stress and inflammation in streptozotocin-induced diabetic rats. Appl Biochem Biotechnol 2022;194(12):6407–22. https://doi.org/10.1007/s12010-022-04012-5.

[14] Li R, Roy R. Gut microbiota and its role in anti-aging phenomenon: evidence-based review. Appl Biochem Biotechnol 2023. https://doi.org/10.1007/s12010-023-04423-y.

[15] Herrala M, Huovinen M, Järvelä E, Hellman J, Tolonen P, Lahtela-Kakkonen M, et al. Micro-sized polyethylene particles affect cell viability and oxidative stress responses in human colorectal adenocarcinoma Caco-2 and HT-29 cells. Sci Total Environ 2023;1(867):161512. https://doi.org/10.1016/j.scitotenv.2023.161512. Apr.

[16] Cobanoglu H, Belivermis M, Sikdokur E, Kilic O, Cayir A. Genotoxic and cytotoxic effects of polyethylene microplastics on human peripheral blood lymphocytes. Chemosphere 2021;272:129805. https://doi.org/10.1016/j.chemosphere.2021.129805.

[17] Dhaka V, Singh S, Anil AG, Sunil Kumar Naik TS, Garg S, Samuel J, et al. Occurrence, toxicity and remediation of polyethylene terephthalate plastics. A review. Environ Chem Lett 2022;20:1777–800. https://doi.org/10.1007/s10311-021-01384-8.

[18] Kim HM, Kang JS. Metabolomic studies for the evaluation of toxicity induced by environmental toxicants on model organisms. Metabolites 2021;11(8):485. https://doi.org/10.3390/metabo11080485.

[19] Olesti E, González-Ruiz V, Wilks MF, Boccard J, Rudaz S. Approaches in metabolomics for regulatory toxicology applications. Analyst 2021;146(6):1820–34. https://doi.org/10.1039/d0an02212h.

[20] Abdul Kadir, Noor Atiqah Aizan, Asmah Rahmat, Jaafar Hawa Ze. Protective effects of tamarillo (cyphomandrabetacea) extract against high fat diet induced obesity in Sprague-Dawley rats. J Obesity 2015:1–8. https://doi.org/10.1155/2015/846041.

[21] Chen K, Zheng X, Feng M, Li D, Zhang H. Gut microbiota-dependent metabolite trimethylamine N-oxide contributes to cardiac dysfunction in western diet-induced obese mice. Front Physiol 2017;8:139. https://doi.org/10.3389/fphys.2017.00139.

[22] Cui A, Hu Z, Han Y, Yang Y, Li Y. Optimized analysis of in vivo and in vitro hepatic steatosis. J Vis Exp 2017;(121):55178. https://doi.org/10.3791/55178.

[23] Zhang Q, Chen XZ, Huang X, Wang M, Wu J. The association between prenatal exposure to phthalates and cognition and neurobehavior of children-evidence from birth cohorts. Neurotoxicology 2019;73:199–212. https://doi.org/10.1016/j.neuro.2019.04.007.

[24] Sun J, Wu X, Gan J. Uptake and metabolism of phthalate esters by edible plants. Environ Sci Technol 2015;49(14):8471–8. https://doi.org/10.1021/acs.est.5b01233.

[25] Li R, Liang J, Gong Z, Zhang N, Duan H. Occurrence, spatial distribution, historical trend and ecological risk of phthalate esters in the Jiulong River, Southeast China. Sci Total Environ 2017;580:388–97. https://doi.org/10.1016/j.scitotenv.2016.11.190.

[26] Kismali G, Yurdakok-Dikmen B, Kuzukiran O, Arslan P, Filazi A. Phthalate induced toxicity in prostate cancer cell lines and effects of alpha lipoic acid. Bratisl Lek Listy 2017;118(8):460–6. https://doi.org/10.4149/BLL_2017_089.

[27] Lu X, Xu X, Lin Y, Zhang Y, Huo X. Phthalate exposure as a risk factor for hypertension. Environ Sci Pollut Control Ser 2018;25(21):20550–61. https://doi.org/10.1007/s11356-018-2367-6.

[28] Trasande L. A global plastics treaty to protect endocrine health. Lancet Diabetes Endocrinol 2022;10(9):616–8. https://doi.org/10.1016/S2213-8587(22)00216-9.

[29] Trasande L, Sathyanarayana S, Spanier AJ, Trachtman H, Attina TM, Urbina EM. Urinary phthalates are associated with higher blood pressure in childhood. J Pediatr 2013;163(3):747–753.e1. https://doi.org/10.1016/j.jpeds.2013.03.072.

[30] Mariana M, Feiteiro J, Verde I, Cairrao E. The effects of phthalates in the cardiovascular and reproductive systems: a review. Environ Int 2016;94:758–76. https://doi.org/10.1016/j.envint.2016.07.004.

[31] Chen H, Feng W, Chen K, Qiu X, Xu H, Mao G, et al. Transcriptomic responses predict the toxic effect of parental co-exposure to dibutyl phthalate and diisobutyl phthalate on the early development of zebrafish offspring. Aquatic toxicology (Amsterdam, Netherlands) 2021;235:105838. https://doi.org/10.1016/j.aquatox.2021.105838.

[32] Su TC, Hwang JJ, Sun CW, Wang SL. Urinary phthalate metabolites, coronary heart disease, and atherothrombotic markers. Ecotoxicol Environ Saf 2019;173:37–44. https://doi.org/10.1016/j.ecoenv.2019.02.021.

[33] Pfuderer P, Francis AA. Phthalate esters: heartrate depressors in the goldfish. Bull Environ Contam Toxicol 1975;13(3):275–9. https://doi.org/10.1007/BF01685335.

[34] Pfuderer P, Janzen S, Rainey WT. The identification of phthalic acid esters in the tissues of cyprinodont fish and their activity as heartrate depressors.

Environ Res 1975;9(3):215–23. https://doi.org/10.1016/0013-9351(75)90002-X.
[35] Mariana M, Cairrao E. Phthalates implications in the cardiovascular system. J Cardiovasc Develop Disease 2020;7(3):26. https://doi.org/10.3390/jcdd7030026.
[36] Jaimes R 3rd, Swiercz A, Sherman M, Muselimyan N, Marvar PJ, Posnack NG. Plastics and cardiovascular health: phthalates may disrupt heart rate variability and cardiovascular reactivity. Am J Physiol Heart Circ Physiol 2017;313(5):H1044–53. https://doi.org/10.1152/ajpheart.00364.2017.
[37] Powell-Wiley TM, Poirier P, Burke LE, Després JP, Gordon-Larsen P, Lavie CJ, et al. Obesity and cardiovascular disease: a scientific statement from the American heart association. Circulation 2021;143(21):e984–1010. https://doi.org/10.1161/CIR.0000000000000973.
[38] Dales RE, Kauri LM, Cakmak S. The associations between phthalate exposure and insulin resistance, β-cell function and blood glucose control in a population-based sample. Sci Total Environ 2018;612:1287–92. https://doi.org/10.1016/j.scitotenv.2017.09.009.
[39] Liang QX, Lin Y, Fang XM, Gao YH, Li F. Association between phthalate exposure in pregnancy and gestational diabetes: a Chinese cross-sectional study. Int J Gen Med 2022;15:179–89. https://doi.org/10.2147/IJGM.S335895.
[40] Castro-Correia C, Correia-Sá L, Norberto S, Delerue-Matos C, Domingues V, Costa-Santos C, et al. Phthalates and type 1 diabetes: is there any link? Environ Sci Pollut Res Int 2018;25(18):17915–9. https://doi.org/10.1007/s11356-018-1997-z.
[41] Radke Elizabeth G, Galizia Audrey, Thayer Kristina A, Cooper Glinda S. Phthalate exposure and metabolic effects: a systematic review of the human epidemiological evidence. Environ Int 2019;132:104768. https://doi.org/10.1016/j.envint.2019.04.040.
[42] Gao H, Zhang C, Tao FB. Association between prenatal phthalate exposure and gestational metabolic syndrome parameters: a systematic review of epidemiological studies. Environ Sci Pollut Res Int 2021;28(17):20921–38. https://doi.org/10.1007/s11356-021-13120-4.
[43] Gao H, Zhu BB, Huang K, Zhu YD, Yan SQ, Wu XY, et al. Effects of single and combined gestational phthalate exposure on blood pressure, blood glucose and gestational weight gain: a longitudinal analysis. Environ Int 2021;155:106677. https://doi.org/10.1016/j.envint.2021.106677.
[44] Han H, Lee HA, Park B, Park B, Hong YS, Ha EH, et al. Associations of phthalate exposure with lipid levels and insulin sensitivity index in children: a prospective cohort study. Sci Total Environ 2019;662:714–21. https://doi.org/10.1016/j.scitotenv.2019.01.151.
[45] Jepsen KF, Abildtrup A, Larsen ST. Monophthalates promote IL-6 and IL-8 production in the human epithelial cell line A549. Toxicol Vitro 2004;18(3):265–9. https://doi.org/10.1016/j.tiv.2003.09.008.
[46] Yang L, Yin W, Li P, Hu C, Hou J, Wang L, et al. Seasonal exposure to phthalates and inflammatory parameters: a pilot study with repeated measures. Ecotoxicol Environ Saf 2021;208:111633. https://doi.org/10.1016/j.ecoenv.2020.111633.
[47] Posnack NG, Swift LM, Kay MW, Lee NH, Sarvazyan N. Phthalate exposure changes the metabolic profile of cardiac muscle cells. Environ Health Perspect 2012;120(9):1243–51. https://doi.org/10.1289/ehp.1205056.
[48] Wen Zeng-Jin, Wang Zhong-Yu, Zhang Yin-Feng. Adverse cardiovascular effects and potential molecular mechanisms of DEHP and its metabolites—a review. Sci Total Environ 2022;847:157443. https://doi.org/10.1016/j.scitotenv.2022.157443.
[49] Chan MM, Yang X, Wang H, Saaoud F, Sun Y, Fong D. The microbial metabolite trimethylamine N-oxide links vascular dysfunctions and the autoimmune disease rheumatoid arthritis. Nutrients 2019;11(8):1821. https://doi.org/10.3390/nu11081821.
[50] Song P, Gao J, Li X, Zhang C, Zhu L, Wang J, et al. Phthalate induced oxidative stress and DNA damage in earthworms (Eisenia fetida). Environ Int 2019;129:10–7. https://doi.org/10.1016/j.envint.2019.04.074.
[51] Cui Y, Li B, Du J, Huo S, Song M, Shao B, et al. Dibutyl phthalate causes MC3T3-E1 cell damage by increasing ROS to promote the PINK1/Parkin-mediated mitophagy. Environ Toxicol 2022;37(10):2341–53. https://doi.org/10.1002/tox.23600.
[52] Jonsson AL, Bäckhed F. Role of gut microbiota in atherosclerosis. Nat Rev Cardiol 2017;14(2):79–87. https://doi.org/10.1038/nrcardio.2016.183.
[53] Fu X, Han H, Li Y, Xu B, Dai W, Zhang Y, et al. Di-(2-ethylhexyl) phthalate exposure induces female reproductive toxicity and alters the intestinal microbiota community structure and fecal metabolite profile in mice. Environ Toxicol 2021;36(6):1226–42. https://doi.org/10.1002/tox.23121.
[54] Mu X, Chen X, Liu J, Yuan L, Wang D, Qian L, et al. A multi-omics approach reveals molecular mechanisms by which phthalates induce cardiac defects in zebrafish (Danio rerio). Environmental pollution (Barking, Essex : 1987) 2020;265(Pt B):113876. https://doi.org/10.1016/j.envpol.2019.113876.
[55] Brawner KM, Yeramilli VA, Duck LW, Van Der Pol W, Smythies LE, Morrow CD, et al. Depletion of dietary aryl hydrocarbon receptor ligands alters microbiota composition and function. Sci Rep 2019;9(1):14724. https://doi.org/10.1038/s41598-019-51194-w.
[56] Higgins AJ, Lees P. The acute inflammatory process, arachidonic acid metabolism and the mode of action of anti-inflammatory drugs. Equine Vet J 1984;16(3):163–75. https://doi.org/10.1111/j.2042-3306.1984.tb01893.x.
[57] Wang B, Wu L, Chen J, Dong L, Chen C, Wen Z, et al. Metabolism pathways of arachidonic acids: mechanisms and potential therapeutic targets. Signal Transduct Targeted Ther 2021;6(1):94. https://doi.org/10.1038/s41392-020-00443-w.
[58] Weiss HJ, Turitto VT. Prostacyclin (prostaglandin I2, PGI2) inhibits platelet adhesion and thrombus formation on subendothelium. Blood 1979;53(2):244–50.
[59] Jugdutt BI, Becker LC. Prostaglandin inhibition and myocardial infarct size. Clin Cardiol 1981;4(3):117–24. https://doi.org/10.1002/clc.4960040302.
[60] Zhang J, Gong Y, Yu Y. PG F(2α) receptor: a promising therapeutic target for cardiovascular disease. Front Pharmacol 2010;1:116. https://doi.org/10.3389/fphar.2010.00116.
[61] Suzuki J, Ogawa M, Watanabe R, Takayama K, Hirata Y, Nagai R, et al. Roles of prostaglandin E2 in cardiovascular diseases. Int Heart J 2011;52(5):266–9. https://doi.org/10.1536/ihj.52.266.
[62] Liu M, Han Q, Yang J. Trimethylamine-N-oxide (TMAO) increased aquaporin-2 expression in spontaneously hypertensive rats. Clin Exp Hypertens 2019;41(4):312–22. https://doi.org/10.1080/10641963.2018.1481420.
[63] Sonnweber T, Pizzini A, Nairz M, Weiss G, Tancevski I. Arachidonic acid metabolites in cardiovascular and metabolic diseases. Int J Mol Sci 2018;19(11):3285. https://doi.org/10.3390/ijms19113285.
[64] Huang CC, Chang MT, Leu HB, Yin WH, Tseng WK, Wu YW, et al. Association of arachidonic acid-derived lipid mediators with subsequent onset of acute myocardial infarction in patients with coronary artery disease. Sci Rep 2020;10(1):8105. https://doi.org/10.1038/s41598-020-65014-z.
[65] Huang YQ, Tang YX, Qiu BH, Talukder M, Li XN, Li JL. Di-2-ethylhexyl phthalate (DEHP) induced lipid metabolism disorder in liver via activating the LXR/SREBP-1c/PPARα/γ and NF-κB signaling pathway. Food Chem Toxicol 2022;165:113119. https://doi.org/10.1016/j.fct.2022.113119.
[66] Yang L, Mäki-Petäjä K, Cheriyan J, McEniery C, Wilkinson IB. The role of epoxyeicosatrienoic acids in the cardiovascular system. Br J Clin Pharmacol 2015;80(1):28–44. https://doi.org/10.1111/bcp.12603.
[67] Brash AR. Arachidonic acid as a bioactive molecule. J Clin Invest 2001;107(11):1339–45. https://doi.org/10.1172/JCI13210.
[68] Lim S, Chang DH, Ahn S, Kim BC. Whole genome sequencing of "Faecalibaculumrodentium" ALO17, isolated from C57BL/6J laboratory mouse feces. Gut Pathog 2016;8:3. https://doi.org/10.1186/s13099-016-0087-3.
[69] Cox LM, Sohn J, Tyrrell KL, Citron DM, Lawson PA, Patel NB, et al. Description of two novel members of the family *Erysipelotrichaceae*: *ileibacterium valens* gen. nov., sp. nov. and *Dubosiella newyorkensis*, gen. nov., sp. nov., from the murine intestine, and emendation to the description of *Faecalibaculum rodentium*. Int J Syst Evol Microbiol 2017;67(5):1247–54. https://doi.org/10.1099/ijsem.0.001793.